

MEASUREMENT OF HEAT-TRANSFER COEFFICIENTS  
IN SHOCK WAVE-TURBULENT BOUNDARY LAYER INTERACTION  
REGIONS WITH A MULTI-LAYERED THIN FILM HEAT TRANSFER GAUGE

Masanori Hayashi, Akira Sakurai and Shigeru Aso

(NASA-TM-77958) MEASUREMENT OF  
HEAT-TRANSFER COEFFICIENTS IN SHOCK  
WAVE-TURBULENT BOUNDARY LAYER INTERACTION  
REGIONS WITH A MULTI-LAYERED THIN FILM HEAT  
TRANSFER (National Aeronautics and Space

N86-21790

Unclas  
G3/34 05706

Translation of "Taso maku netsusoku sensa ni yoru  
shogekiharanryu kyokaiso kanshoiki ni okeru netsu-  
dendo keisu no sokutei", Faculty of Engineering,  
Kyushu University, Memoirs of the Faculty of Engin-  
eering, Technology Reports, Vol. 57, August 1984,  
pp. 455-462



## STANDARD TITLE PAGE

1. Report No. NASA TM-77958	2. Government Accession No.	3. Recipient's Catalog No.
4. Title and Subtitle Measurement of Heat-Transfer Coefficients in Shock Wave-Turbulent Boundary Layer Interaction Regions with a Multi-Layered Thin Film Heat Transfer Gauge		5. Report Date January 1986
		6. Performing Organization Code
7. Author(s) Masanori Hayashi, Akira Sakurai and Shigeru Aso		8. Performing Organization Report No.
		10. Work Unit No.
9. Performing Organization Name and Address SCITRAN Box 5456 Santa Barbara, CA 93108		11. Contract or Grant No. NASw- 3542
12. Sponsoring Agency Name and Address National Aeronautics and Space Administration Washington, D.C. 20546		13. Type of Report and Period Covered Translation
		14. Sponsoring Agency Code
15. Supplementary Notes Translation of "Taso maku netsusoku sensa ni yoru shogekiharanryu kyokaiso kanshoiki ni okeru netsudendo keisu no sokutei", Faculty of Engineering, Kyushu University, Memoirs of the Faculty of Engineering, Technology Reports, Vol. 57, August 1984, pp. 455-462. (A85-20997)		
16. Abstract  A new type of thin film heat transfer gauge is applied to the measurement of heat-transfer coefficients in the interaction regions of incident shock waves and fully developed turbulent boundary layers. It has been developed to measure heat flux with high spatial resolution and fast response for wind tunnels with long flow duration. To measure the heat-transfer coefficients in the interaction region in detail, experiments were performed under the conditions of Mach number = 4, total pressure = 1.2 MPa, $T_w/T_o = 0.59 \sim 0.65$ , Reynolds number = $1.3 \sim 1.5 \times 10^7$ , and incident shock angles from $17.8^\circ$ to $22.8^\circ$ . The results show that the heat-transfer coefficient changes complicatedly in the interaction region. At the beginning of the interaction region, the heat-transfer coefficient decreases at first, reaches its minimum value at the point where the pressure begins to increase, and then increases sharply. When the boundary layer begins to separate, even a small separation bubble causes significant changes in the heat-transfer coefficient, while the pressure does not show any change which suggests that the boundary layer begins to separate.		
17. Key Words (Selected by Author(s))		18. Distribution Statement  Unclassified - Unlimited
19. Security Classif. (of this report) Unclassified	20. Security Classif. (of this page) Unclassified	21. No. of Pages 16
		22. Price

ORIGINAL PAGE IS  
OF POOR QUALITY

# Measurement of Heat-Transfer Coefficients in Shock Wave-Turbulent Boundary Layer Interaction Regions with a Multi-Layered Thin Film Heat Transfer Gauge.

\* /455

Masanori Hayashi, Akira Sakurai and Shigeru Aso

## 1. Introduction.

It is a well known problem in aero-engineering that in a supersonic aircraft such as the Space Shuttle, shock waves interact with turbulent boundary layers of the aircraft surface and a large local heat-flux is generated by separation and reattachment of the boundary layer.<sup>1)</sup>

Although many experiments have been performed on this problem,<sup>2)-4)</sup> detailed measurement of heat-flux is not available due to enormous spatial variations of heat-flux and pressure in the interaction regions. Therefore, the mechanism of air-friction heating and detailed structures of heat-flux are not well known.

In order to measure heat-flux of the interaction regions, we have developed a heat transfer gauge with good spatial resolution and fast response. This gauge can be used in a supersonic wind tunnel with long flow duration as well as in a shock wave tube with short flow duration. Measurement theory, methods to make the gauge, and method of calibration have been already reported.<sup>5)</sup> This gauge directly measures heat-flux by measuring temperature gradient of a thermal resistor using two thin metal films.

We have applied this gauge to the heat-flux measurement in the interaction regions of incident shock waves and turbulent boundary layer, and proved that the gauge has high sensitivity and good resolution.<sup>6)</sup> In the present experiment, the gauge was applied to the measurement of heat-transfer coefficients in the interaction regions of shock wave and turbulent boundary layer.

## 2. Multi-layered thin film heat transfer gauge.

\456

A schematic structure of the multi-layered thin film heat-transfer gauge is shown in Fig. 1. A layer of thermal resistor is attached on the object surface

---

\* Numbers in margin indicate pagination of foreign text.

through an electrical insulator. The heat-flux measurement is made by measuring temperature gradient of the thermal resistor layer using two thin metal film thermometers ("thin film gauge" in short) attached on both sides of the surface. These films are made by vacuum evaporation. Silicon-monoxide is used for the electrical insulator and the thermal resistor layer, and Nickel is used for the thin film gauge. The thin film gauge used in the present experiment is shown in Fig. 2 and its width is 0.2 mm. Spatial resolution of the gauge is 0.2 mm; frequency response is about 600 Hz; and sensitivity is  $2.10 \times 10^{-9} \text{ V}/(\text{W}/\text{m}^2)$  for 1 V bridge voltage. The detailed explanation of the measurement theory and the calibration method are described in ref. 6).

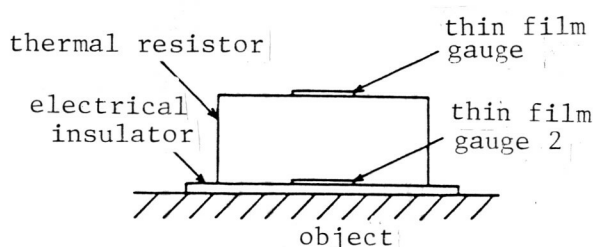


Figure 1. Schematic structure of the multi-layered thin film heat-transfer gauge.



Figure 2. The thin film gauge used in the experiment.

### 3. Experimental setup and method.

A turbulent boundary layer is created on a plate model located in a supersonic wind tunnel. A shock wave generator is placed in front of the model and an interaction region is created by introducing the shock wave onto the boundary layer. In principle, many gauges can be placed in the main stream and many measurements can be made simultaneously. In the present experiment, however, one gauge was used by moving the shock wave generator along the main stream, because a steady flow lasting for about a minute was available in the wind tunnel.

#### 3.1 Experimental setup.

The supersonic wind tunnel used in the experiment has the following charac-

\ 457



\ 457

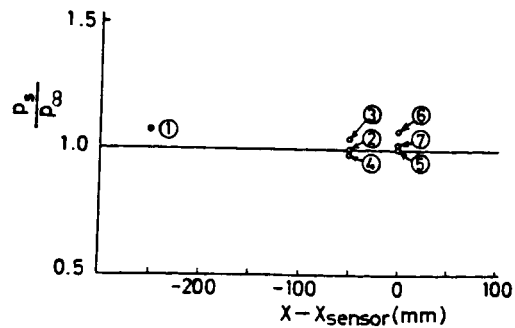


Figure 4. Pressure distribution on the plate.

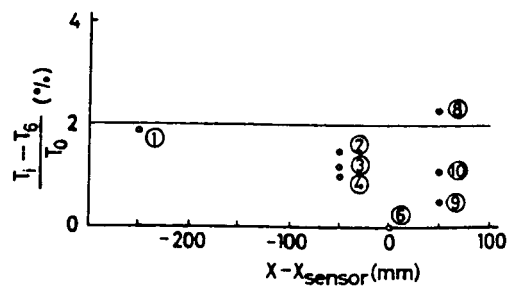


Figure 5. Temperature distribution on the plate.

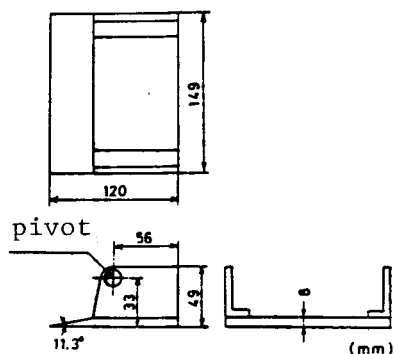


Figure 6. The shock wave generator.

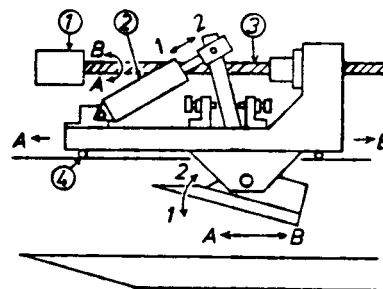


Figure 7. The moving and angle varying mechanisms of the shock wave generator.

- (1) stepping motor
- (2) air-actuator
- (3) ball screws
- (4) linear motion bearings

The shock wave generator used in the experiment is shown in Fig. 6. Since the wind tunnel can not be started if the wedge angle of the shock wave generator is large, the wedge angle is set to zero degrees at first. After starting the wind tunnel, the wedge angle is increased by an actuator. The movement of the device along the main stream is made by a stepping motor and ball screws with a positioning accuracy of 0.01 mm. Flexure of the shock wave generator holder is under 0.1 mm during the wind tunnel operation. The moving and angle varying mechanisms are shown in Fig. 7. The moving range along the main stream is  $\pm 62$  mm. Since the distance between the leading edge of the plate and the measuring gauge is 500 mm, there is almost no variation in the Reynolds number based on the distance between the leading edge of the plate and the shock wave impact point.

### 3.2 Experimental conditions.

The experimental conditions are shown in Table 1. Reynolds number is based on the distance between the leading edge of the plate and the measuring gauge. The incident shock angles were measured by the Schlieren photography.

TABLE 1. Experimental conditions

incident shock angle	Mach no.	$M_\infty$	pressure $P_0$ ( $\times 10^6$ Pa)	temp. $T_0$ (K)	$Re_x$	relative wall temp. $T_w/T_0$
17.8°	4.00		1.23	479	$1.36 \times 10^7$	0.617
18.5°	4.00		1.23	490	$1.31 \times 10^7$	0.602
19.2°	3.99		1.23	490	$1.32 \times 10^7$	0.603
20.2° (Case1)	3.98		1.21	447	$1.50 \times 10^7$	0.655
20.2° (Case2)	3.99		1.22	480	$1.35 \times 10^7$	0.615
21.2°	3.98		1.24	460	$1.47 \times 10^7$	0.640
21.5°	3.99		1.24	506	$1.27 \times 10^7$	0.585
22.4°	4.05		1.22	493	$1.26 \times 10^7$	0.601
22.8°	3.98		1.22	470	$1.40 \times 10^7$	0.628

### 3.3 Experimental method.

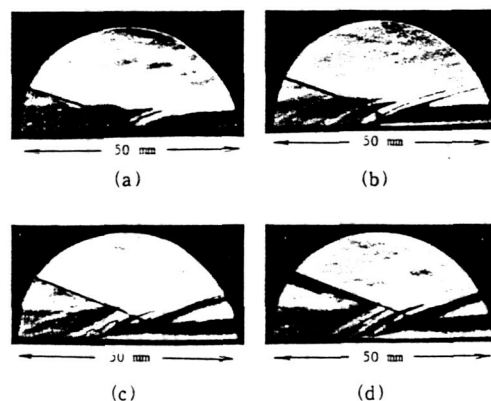
After the wind tunnel became a stationary state, the shock wave genera-

tor was moved with a constant velocity (3 mm/sec). The angle and movement controls were made by a microcomputer. All the readings of heat-flux gauges, pressure sensors, and thermocouples were recorded using a 12 bit-AD converter. The spatial resolution was less than 0.5 mm. The coordinate of the pressure and heat-transfer distributions along the main stream is defined such that the origin is the impact point of the shock wave on the plate and the positive direction is along the main stream.

#### 4. Results and considerations.

##### 4.1 Visualization of the stream.

Typical Schlieren photographs of the interaction region are shown in Fig. 8(a)-(d). The knife edge is horizontal to the plate.



- (a) incident shock angle  $18.5^\circ$
- (b) incident shock angle  $20.2^\circ$  (Case 1)
- (c) incident shock angle  $20.2^\circ$  (Case 2)
- (d) incident shock angle  $22.1^\circ$

Fig. 8 Schlieren photographs (The left hand side is upstream).

At the incident shock angle  $18.5^\circ$ , the incident shock wave is bent gradually and reflected in the boundary layer. Compressive waves are observed in front of the reflected shock wave.

Since the incident shock angle  $20.2^\circ$  corresponds to the transition angle where the boundary layer starts to separate as described in section 4.3, various wave forms and different pressure distributions are observed due to small differences of the experimental conditions. For convenience, Fig. 8(b) (corresponding pressure distribution is Fig. 11(a)) will be called Case 1, and Fig. 8(c) (corresponding pressure distribution is Fig. 12(a)) will be called Case 2. In Case 1, similar wave forms observed in shock angle  $18.5^\circ$  are observed. In Case 2, however, the shock wave crosses the reflected shock wave around the impact point to the boundary layer. Reflected expansive waves are also observed.

For the incident shock angles greater than  $21.2^\circ$ , the reflected shock wave is observed in front of the impact point as shown in Fig. 8(b). Area of the reflected expansive waves created behind the reflected waves is also increased.

#### 4.2 Pressure distribution.

Typical pressure distributions in the interaction region are shown in Fig. 9(a) to Fig. 13(a). The pressure is normalized to that on the wind tunnel wall.

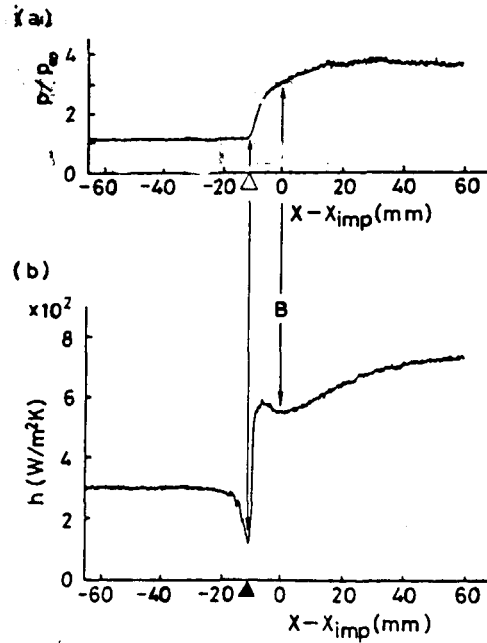


Figure 9. At the incident shock angle  $18.5^\circ$ .

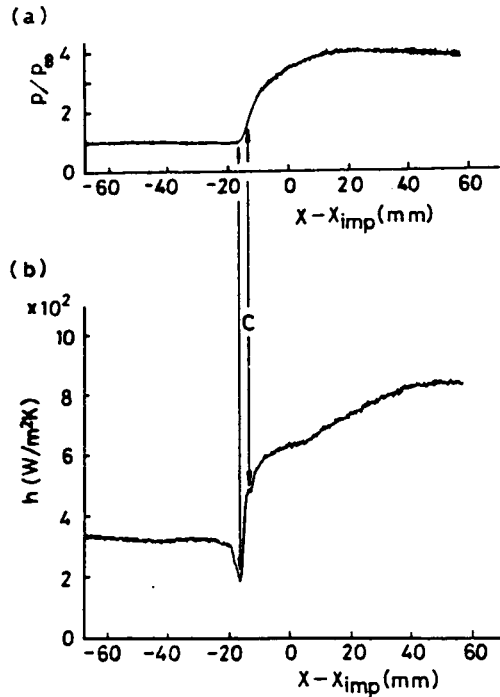


Figure 10. At the incident shock angle  $19.2^\circ$   
(a) pressure distribution (b) heat-transfer coefficient distribution

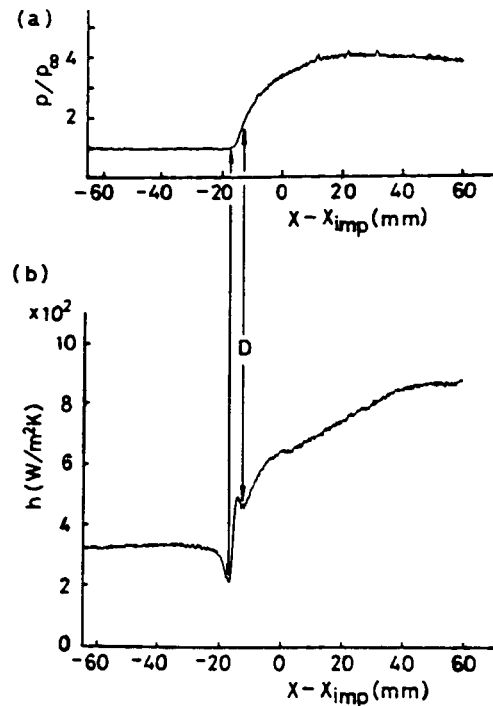


Figure 11. At the incident shock angle  $20.2^\circ$  (case 1)  
(a) pressure distribution (b) heat-transfer coefficient distribution

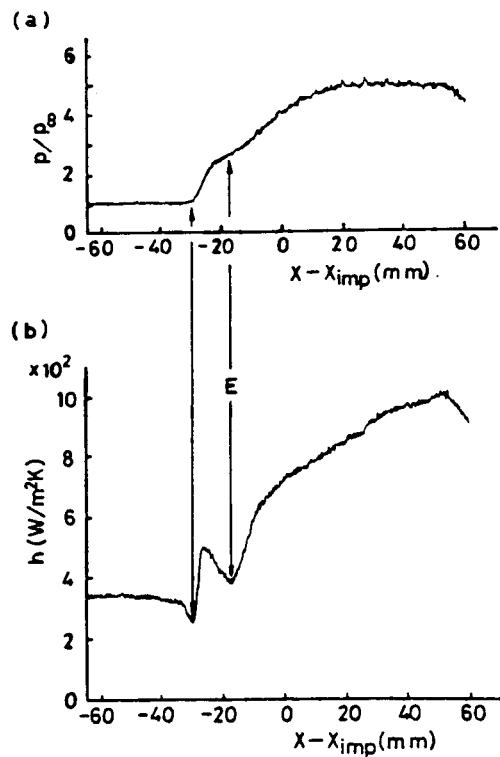


Figure 12. At the incident shock angle  $20.2^\circ$  (case 2)  
(a) pressure distribution (b) heat-transfer coefficient distribution

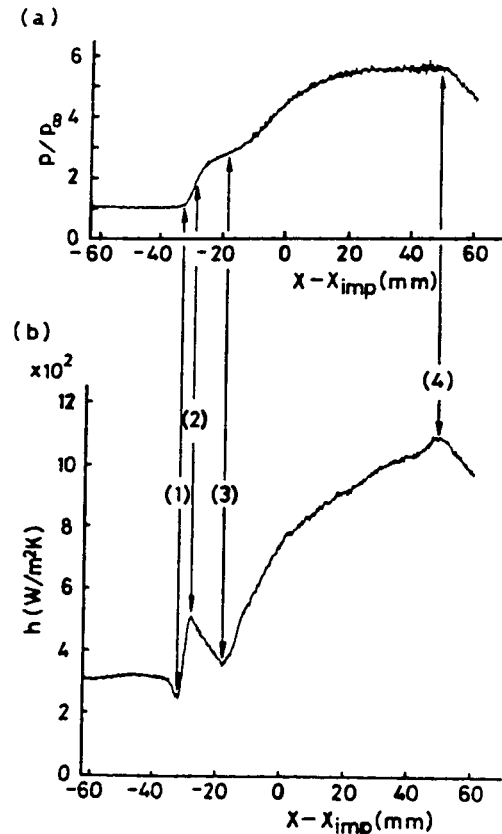


Figure 13. At the incident shock angle  $22.1^\circ$   
(a) pressure distribution (b) heat-transfer coefficient distribution

From the shock angle  $17.8^\circ$  to  $19.2^\circ$ , the pressure increases rapidly in front of the impact point to the boundary layer and, then gradually reaches a constant value.

At shock angle  $20.2^\circ$ , the pressure distribution of Case 1 shows a similar behavior observed in the angles between  $17.8^\circ$  and  $19.2^\circ$ . The pressure distribution of Case 2, however, shows a different behavior. Namely, a plateau is observed after the rapid increase. The plateau is a characteristic behavior of the boundary layer separation in the interaction region.<sup>7),8)</sup> This plateau region seems to be expanding as the shock angle increases up to  $22.8^\circ$ .

It is known from the previous experiments of shock wave and boundary layer interaction that the boundary layer starts to separate at the beginning of the plateau region and reattaches at the end where the pressure starts increasing again.<sup>7),8)</sup> Therefore, at the shock angles greater than  $20.2^\circ$  where the plateau is observed, the boundary layer starts to separate at the beginning of the plateau region and reattaches at the end. However, the appearance of pressure plateaus is not necessarily related to very small separation bubbles as described in the next section of the heat-transfer coefficient measurement.

#### 4.3 Heat-transfer coefficient distribution.

The heat-transfer coefficient distribution in the interaction region was measured in terms of the following value  $h$ :<sup>3)</sup>

$$h = \frac{q_w}{T_{aw} - T_w},$$

where

$$T_{aw} = T_\infty \left( 1 + R \cdot \frac{\gamma - 1}{2} M_\infty^2 \right),$$

\460

$$R = \sqrt[3]{P_\gamma}.$$

Prandtl number  $P_\gamma$  is calculated at the wall temperature  $T_w$ .

Typical heat-transfer coefficient distributions in the interaction region are shown in Fig. 9(b) - Fig. 13(b). Since the heat-transfer coefficients were measured with good spatial resolution, interesting results have been obtained.

As shown in Fig. 9(b)-13(b), it is found for all incident shock angles that the heat-transfer coefficient decreases to a minimum just before the shock wave enters the boundary layer, and then increases rapidly. For the shock angle  $18.5^\circ$ , the minimum of the heat-transfer coefficient occurs at the point shown with  $\triangle$  in Fig. 9(b) which corresponds to the point where the pressure starts increasing as shown with  $\triangle$  in Fig. 9(a). This means that the heat-transfer coefficient starts decreasing before the pressure starts increasing. This phenomenon is observed experimentally for the first time.

Although Holden<sup>2)</sup>, and Kaufman II and Johnson<sup>3)</sup> have reported a similar reduction of the heat-transfer coefficient in the interaction region of shock wave and boundary layer, our experiment has made more detailed observations such as location of minimum, magnitude and variation of the heat-transfer coefficient, and relation between pressure and heat-transfer distributions.

Appearance of the minimum of heat-transfer coefficient may be explained as follows. A reversed pressure gradient is created in the boundary layer by the interaction of compressive wave and reflected shock wave. While the boundary layer crosses the pressure gradient, the velocity gradient and, therefore, surface friction near the surface get reduced, resulting in the reduction of air-friction heating. Back and Cuffel<sup>4)</sup> have observed the reduction of velocity gradient of the boundary layer in interaction regions.

Behavior of the heat-transfer coefficient after the rapid increase was observed as follows. For the shock angles between  $17.8^\circ$  and  $20.2^\circ$  (Case 1), the pressure

distribution did not change, but the heat-transfer coefficient changed greatly. At the shock angles  $17.8^\circ$  and  $18.5^\circ$ , after reaching the peak value, the heat-transfer coefficient decreased slightly and, then increased gradually reaching to the maximum value. At the shock angle  $19.2^\circ$ , the heat-transfer coefficient distribution shows a break during the rapid increase. At the shock angle  $20.2^\circ$  (Case 1), this break developed to a dip as shown in Fig. 11(b). This tendency is even pronounced in Case 2 as shown in Fig. 12(b). On the other hand, the pressure distribution of Case 2 clearly shows a difference from that of smaller shock angles, as shown in Fig. 11(a) and 12(b). It is worth mentioning that the plateau of pressure distribution is not yet appeared at the shock angles  $19.2^\circ$  and  $20.2^\circ$  (Case 1), but the heat-transfer coefficient behavior observed at the shock angles larger than  $20.2^\circ$  (Case 2) already appeared at  $19.2^\circ$  and  $20.2^\circ$  (case 1). Since the first peak position of the heat-transfer coefficient corresponds to the point where the boundary layer starts to separate, the boundary layer starts to separate around shock angle  $19.2^\circ$ , and small separation bubbles are developed at shock angle  $20.2^\circ$  Case 1. The shock angles between  $19.2^\circ$  and  $20.2^\circ$  correspond to the transitional region of the boundary layer separation. \ 461

For the shock angles between  $20.2^\circ$  (Case 2) and  $22.8^\circ$ , the heat-transfer coefficient distributions show a similar behavior as shown in Fig. 12(b) - 13(b). Typical behavior will be explained as follows taking Fig. 13(b) as an example.

The heat-transfer coefficient reaches a minimum value at the point when the pressure starts increasing (1), and then increases rapidly to a maximum value just before the pressure plateau starts (2). After the maximum, the heat-transfer coefficient decreases until the pressure plateau ends, and then increases again (3) until far beyond the interaction region (from (3) to (4)). Although it is not directly related to the interaction phenomena, the heat-transfer coefficient decreases rapidly at the far end due to the expansive wave coming from the back of the shock wave generator (4).

The phenomenon of rapid increase of the heat-transfer coefficient after the

minimum is due to the same reason described above for the case where the boundary layer is not separated. The point where the heat-transfer coefficient is maximum corresponds to the point where the boundary layer starts to separate. Therefore, in the downstream side of this point, the air-friction heating and the heat-transfer coefficient are reduced. In the region where the heat-transfer coefficient is decreasing (between (2) and (3)), the pressure plateau region is spreading and the shock wave strength is increasing.

As mentioned earlier, the boundary layer re-attaches when the pressure starts increasing after the plateau. The heat-transfer coefficient starts increasing slightly before the end of the pressure plateau, and still keeps increasing after the pressure has reached to the maximum. This is because in the downstream of the point where the boundary layer reattaches, the stream is bent toward the surface by the reflected expansive wave and the air-friction heat is generated.

In this experiment, we showed that the heat-transfer coefficient changes complicatedly for both cases where boundary layer is separated and not separated, and studied the detailed mechanism of air-friction heating in the interaction region. It is found that in the interaction region of shock wave and boundary layer, a large heat load is generated because of the large variation of local heat-flux.

## 5. Conclusions.

In the present experiment, detailed measurement of the heat-transfer coefficient in interaction region of shock wave and boundary layer has been made using multi-layered thin film heat-flux gauge, and the mechanism of air-friction heating phenomenon in the interaction region has been investigated. The measurement using the heat-flux gauge has been proven to be powerful method for the heat-transfer coefficient measurement which requires good spatial resolution and fast response.

Summary of the experiment is as follows:

(1) Experimental conditions of the interaction region of shock wave and boundary layer: Mach number 4, relative wall temperature ratio  $T_w/T_0 = 0.59$

- 0.66, Reynolds number  $1.2 - 1.5 \times 10^7$ . From the shock angle  $17.8^\circ$  to  $22.8^\circ$ , the heat-transfer coefficient starts decreasing before the pressure increases, and reaches a minimum value.

(2) The shock angles between  $19.2^\circ$  and  $20.2^\circ$  correspond to a transitional region where the boundary layer starts to separate. The pressure distribution is different from the case where the boundary layer is fully separated. On the other hand, the heat-transfer coefficient distribution shows the same behavior, and also shows an indication of small separation bubbles.

(3) In the case where the boundary layer is separated, the heat-transfer coefficient distribution shows complicated behavior. Namely, the coefficient decreases at first and increases rapidly, reaching a maximum value at the point where the boundary layer starts to separate. After the maximum, the coefficient gradually decreases until the pressure plateau ends, and then increases again.

We thank M. Orino and A. Ogawa for their help.

#### Reference

#### REFERENCES

- 1) Korkegi, R. H.: Survey of Viscous Interactions Associated with High Mach. Number Flight. AIAA J., Vol. 19, No. 5 (1971) pp 771-784.
- 2) Holden, M. S.: Shock Wave-Turbulent Boundary Layer Interaction in Hypersonic Flow, AIAA Paper. No. 72-74 (1972).
- 3) Kaufman, II, L. G. and Johnson, C. B.: Interference Heating from Interactions of Shock Waves with Turbulent Boundary Layers at Mach. 6, NASA TN D-7649 (1974).
- 4) Back, L. H. and Cuffel, R. F.: Shock Wave/Turbulent Boundary Layer Interactions with and without Surface Cooling, AIAA J. Vol. 14, No. 4(1976), pp 526-532.
- 5) M. Hayashi, A. Sakurai, K. Aso and S. Aso. "Multi-layered thin film heat transfer gauge", Memoirs of the Faculty of Engineering /462 Kyushu University, Vol. 55, No. 1 (1984).
- 6) Hayashi, M., Sakurai, A. and Aso, S.: An Investigation of a Multi-layered Thin Film Heat Transfer Gauge, Memoirs of the Faculty of Engineering, Kyushu University, Vol. 44, No. 1 (1984).
- 7) Green, J. E.: Interactions between Shock Waves and Turbulent Boundary Layers, Progress in Aerospace Sciences, Vol. 11, Pergamon Press, Oxford (1970), pp. 235-340.
- 8) Reda, D. C. and Murphy, J. D.: Sidewall Boundary-Layer Influence on Shock Wave/Turbulent Boundary Layer Interactions, AIAA J. Vol. 11 No. 10(1973), pp. 1367-1368.